Physica C 479 (2012) 167–169

Contents lists available at SciVerse ScienceDirect

Physica C

journal homepage: www.elsevier.com/locate/physc

1D superconductivity in porous Nb ultrathin films

M. Trezza [a,*], S.L. Prischepa [b], C. Cirillo [a], C. Attanasio [a]

[a] CNR-SPIN Salerno and Dipartimento di Fisica, "E. R. Caianiello", Università degli Studi di Salerno, Via Ponte don Melillo, Fisciano (Sa) I-84084, Italy
[b] State University of Informatics and RadioElectronics, P. Brovka Street 6, Minsk 220013, Belarus

ARTICLE INFO

Article history:
Accepted 2 January 2012
Available online 28 January 2012

Keywords:
Vortex lattices
Nanowires
Porous silicon

ABSTRACT

We report on the measurements of the transport properties of superconducting Nb ultrathin bridges grown by UHV magnetron sputtering on porous Si substrates. The films are about 10 nm thick and inherit from the substrate a structure made of holes with diameter of 10 nm and interpore spacing in the range 20–40 nm. Due to their reduced dimensions, they are sensitive to thermal fluctuations typical of 1D superconductors and exhibit a nonzero resistance below the superconducting transition temperature, T_c. Clear hysteresis and finite jumps in the *I*–*V* curves are also observed.

1. Introduction

With the rapid development of nanotechnology, superconductivity in one dimensional (1D) nanowires has attracted considerable attention in the last two decades [1–9]. The central challenge in the study of thin superconducting wires is to understand how the superconductivity is affected when approaching the 1D limit. Continual advances in the fabrication techniques have allowed researchers to create wires of ever shrinking size, resulting in an increasing number of observed effects that shed light on this basic question. Earlier studies have predicted that, when the wire width is comparable with its superconducting coherence length $\xi(T)$, intrinsic thermal [4,10] and quantum [5,11,12] fluctuations play an increasingly important role, causing the wires to remain resistive much below the superconducting transition temperature T_c with phase slip processes responsible for this phenomenon. At high temperatures (but below T_c) this resistance is caused by thermally activated phase slips (TAPS), in which the system makes a transition across a potential barrier between two different metastable states. At sufficiently low temperatures the general expectation is that the system would tunnel through the barrier between two metastable states, constituting a quantum phase slip event (QPS).

Recently a radically different approach to nanostructures fabrication based on self-assembled growth, such as chemically anisotropic etching of single crystals, has attracted much attention also in the superconducting nanowire field. These processes are useful for generating low-cost simple patterns of nanostructures in a single step, assuring a high reproducibility as well [3,13,14].

In this work we present experimental results obtained on superconducting Nb ultrathin films grown on porous Si substrates. The films are about 10 nm thick and inherit from the substrate a structure made of pores with 10-nm diameter and interpore distance between 20 and 40 nm. Typical features of 1D superconductivity such as non zero resistance below T_c as well as hysteresis and finite jumps in the *I*–*V* characteristics have been observed in our samples.

2. Fabrication

Porous layers have been fabricated by electrochemical anodic etching of n-type, 0.01 Ωcm, monocrystalline silicon wafers. The electrochemical dissolution has been performed in 48% water solution of HF, applying a current density of 20 mA/cm^2. The anodization time was chosen in the range of 0.5–4 min in order to get porous layers with a thickness ranging from 0.5 to 4 μm. The pores extend on a surface of about 1 cm^2. The integral porosity has been estimated by gravimetry to be of about 50% [15]. The resulting porous substrates have diameter Ø = 10 nm and interpore spacing (center–center distance) a_0 = 20–40 nm. Nb thin films have been grown on top of the porous Si substrates in an UHV dc diode magnetron sputtering system with a base pressure in the low 10^{-8} mbar regime and sputtering Argon pressure of 3.5×10^{-3} mbar. In order to reduce the possible contamination present in the porous templates, the substrates have been heated at 120 °C for 1 h in the UHV chamber. The deposition was then realized at room temperature after the cool off of the substrates. The films have been deposited at typical rates of 0.33 nm/s, controlled by a quartz crystal monitor calibrated by low-angle X-ray reflectivity measurements. In this way, an array of interconnected superconducting wires was formed on the substrates, the single wire width, *l*, being the distance between the edges of two consecutive

* Corresponding author.
E-mail address: trezza@sa.infn.it (M. Trezza).

0921-4534/$ - see front matter
doi:10.1016/j.physc.2012.01.001

pores. Therefore is $l = 10$ nm (30 nm) for the sample grown on the substrate with $a_0 = 20$ nm (40 nm). It is worth to underline that the single wire width, l, is comparable with the zero-temperature superconducting coherence length of our samples, $\xi(0) \simeq 10$ nm [16]. Since the effect of the periodic template would be reduced when the film thickness, d_{Nb}, exceeds the pore diameter, Ø [16,17], the Nb thickness was chosen to be in the range of 9–12 nm. Finally, a typical four-probe geometry has been realized on the samples by using standard optical lithography. The dimensions of the obtained bridges were $w = 10$–20 µm for the width and $L = 100$ µm for the length.

3. Experimental results and discussion

All the Nb films deposited on porous Si, their names and thicknesses, as well as the substrate characteristics are summarized in Table 1. For the sake of clarity the samples were named using the initials Si followed by a number indicating the nominal interpore distance, a_0, Nb by a number indicating the Nb thickness and by another number for the bridge width. For example, Si40–Nb12–w20 is the porous Nb bridge 20 µm wide and 12 nm thick, grown on the porous substrate with $a_0 = 40$ nm. From the a_0, Ø and w values of the analyzed samples we can estimate the number of the interconnected wires present in each bridge which are 330 for Si20–Nb9–w10, 200 for Si40–Nb10–w10 and 400 for Si40–Nb12–w20. The numbers listed above are likely to be corrected considering a deviation from the corresponding mean interpore distance of the order of 10% [16].

3.1. Resistive transition

Superconducting nanowires never show zero resistance, although resistance does decrease exponentially upon cooling [6]. The origin of this resistive behavior lies in the occurrence of thermally activated slips of the phase of the Ginzburg–Landau order parameter. During a phase slip, a small normal segment appears on the nanowire for a short time causing the loss of phase coherence [18].

Table 1
Characteristics of porous Si templates and properties of Nb films deposited on such substrates. a_0 indicates the interpore spacing, d_{Nb} the Nb thickness, w the bridge width, T_c the critical temperature. The pore diameter Ø is 10 nm for all the samples.

Sample	a_0 (nm)	d_{Nb} (nm)	w (µm)	T_c (K)
Si20–Nb9–w10	20	9	10	3.60
Si40–Nb10–w10	40	10	10	4.23
Si40–Nb12–w20	40	12	20	3.87

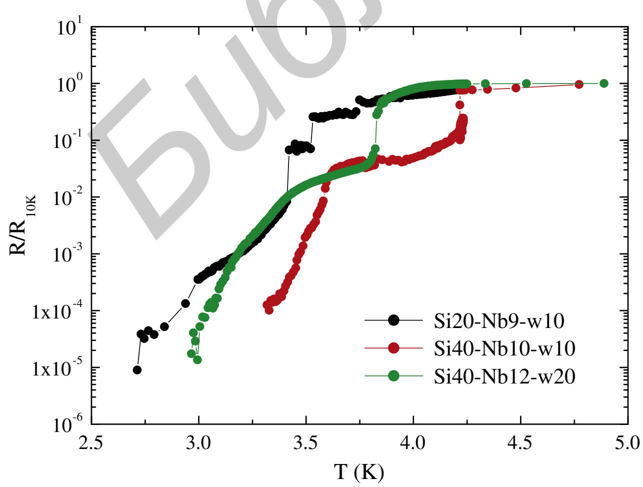

Fig. 1. $R(T)$ transition curves, normalized to the resistance at 10 K, of Nb thin bridges of different widths and thicknesses grown on the porous substrates Si20 and Si40.

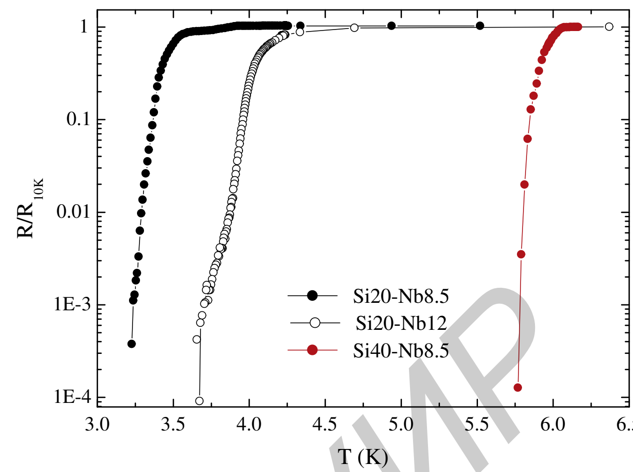

Fig. 2. $R(T)$ transition curves, normalized to the resistance at 10 K, of plane porous Nb films of different thicknesses grown on the porous substrates Si20 and Si40.

In Fig. 1 are reported the $R(T)$ transition curves, normalized to the resistance at 10 K, of porous Nb bridges of different widths and thicknesses grown on the porous substrates Si20 and Si40, namely samples Si40–Nb10–w10 and Si40–Nb12–w20.

For each curve, we observe a first resistance drop at higher temperature which corresponds to the superconducting transition of the larger Nb porous electrodes [4,19]. The resistance value immediately below this drop is taken as the normal resistance R_N of the interconnected wires. The critical temperature values estimated at the midpoint of the $R(T)$ transition curves are reported in Table 1. Moreover, it can be observed that the samples exhibit a nonzero resistance over a large temperature range. The width of the resistance transitions, defined as $\Delta T_c = T_c^{90\%R_N} - T_c^{10\%R_N}$, reaches in fact values up to 0.6 K for the sample Si20–Nb9–w10, namely in the case of the narrowest values. Moreover, it is worth to underline that the resistance of the samples drops about four orders of magnitude within this temperature range below T_c. These curves are significantly broader than the ones observed in similar plane porous Nb films [16], reported, for sake of comparison, in Fig. 2, where $\Delta T_c \sim 0.2$ K. These films were also grown on porous Si substrates but, since they were unpatterned, a much larger number of interconnected superconducting wires are present. For this reason, the superconducting properties, typical of 1D systems, were not observed on such plane films. Therefore, the 1D character of our system is more evident when few interconnected wires are present. Moreover this comparison makes us confident to exclude that sample dishomogeneity (i.e. granularity) can be responsible of the $R(T)$ broadening [20].

3.2. I–V measurements

I–V characteristics have been measured at different temperatures and magnetic fields under current drive condition. The magnetic field was applied perpendicularly to the plane of the substrate. During the measurement the temperature stabilization was around 1 mK. In order to minimize any heating effect the bridges have been kept in contact with liquid helium. The current biasing has been realized by sending rectangular current pulses to the samples, with the current-on time being of 12 ms followed by a current-off time of 1 s. Any single voltage value has been acquired at the maximum value of the current. Here we report the current–voltage characteristics for the sample Si20–Nb9–w10, which

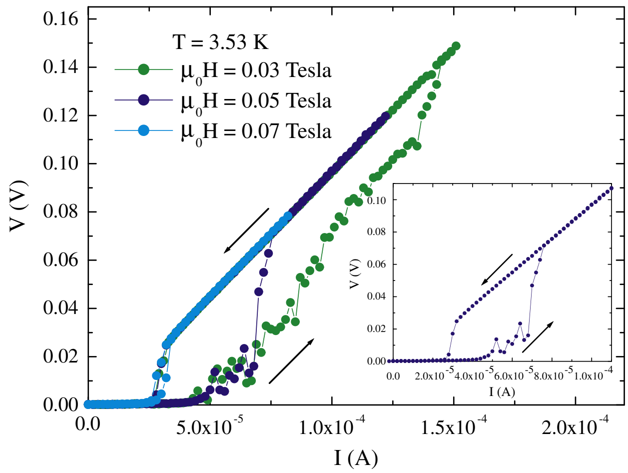

Fig. 3. Current–voltage characteristics of the sample Si20–Nb9–w10 at different applied magnetic fields and at $T = 3.53$ K. The inset is an enlargement of the I–V measurement at μ_0H = 0.05 Tesla.

shows the maximum value of ΔT_c. In Fig. 3 I–V curves measured at different applied magnetic fields and at the temperature of 3.53 K, are shown. All the curves were recorded sweeping the current up and down and clear hysteresis has been detected. Finite jumps were also observed, as highlighted in the inset of Fig. 3, providing further evidence that phase slip phenomena are present since each jump corresponds to phase slip lines entering the sample [21,22]. When the current is swept down a continuous behavior is found without any jump between different resistive states. On the contrary, during the sweeping up we can notice that the voltage progression is peaked instead of following monotonic steps [21,22]. We believe that such behavior is related to the fact that in the interconnected wires there is a competition between 1D and non-1D superconductivity [23].

4. Conclusions

We have studied transport properties of superconducting Nb ultrathin bridges grown on porous Si substrates where the pore diameter is 10 nm and the interpore spacing is 20–40 nm. The samples exhibit a nonzero resistance over a broad temperature range and clear hysteresis with finite jumps in the I–V curves. All these features are more pronounced in the sample Si20–Nb9–w10 which is characterized by the narrowest value of the single superconducting wire widths. All these observations are typical of 1D superconductivity.

References

[1] A.V. Herzog, P. Xiong, F. Sharifi, R.C. Dynes, Phys. Rev. Lett. 76 (1996) 668.
[2] P. Xiong, A.V. Herzog, R.C. Dynes, Phys. Rev. Lett. 78 (1997) 927.
[3] D.Y. Vodolazov, F.M. Peeters, L. Piraux, S. Mátéfi-Tempfli, S. Michotte, Phys. Rev. Lett. 91 (2003) 157001.
[4] A. Rogachev, A.T. Bollinger, A. Bezryadin, Phys. Rev. Lett. 94 (2005) 017004.
[5] M.L. Tian, N. Kumar, S.Y. Xu, J.G. Wang, J.S. Kurtz, M.H.W. Chan, Phys. Rev. Lett. 95 (2005) 076802.
[6] K.Y. Arutyunov, D.S. Golubev, A.D. Zaikin, Phys. Rep. 464 (2008) 1.
[7] M. Zgirski, K.P. Riikonen, V. Touboltsev, K. Arutyunov, Nano Lett. 5 (2005) 1029.
[8] F. Altomare, A.M. Chang, M.R. Melloch, Y.G. Hong, C.W. Tu, Phys. Rev. Lett. 97 (2006) 017001.
[9] X.Y. Bao, Y.F. Zhang, Y.P. Wang, J.F. Jia, Q.K. Xue, X.C. Xie, Z.X. Zhao, Phys. Rev. Lett. 95 (2005) 247005.
[10] D.E. McCumber, B.I. Halperin, Phys. Rev. B 1 (1970) 1054.
[11] N. Giordano, Phys. Rev. Lett. 61 (1988) 2137.
[12] A.D. Zaikin, D.S. Golubev, A. van Otterlo, G.T. Zimanyi, Phys. Rev. Lett. 78 (1997) 1552.
[13] S. Michotte, L. Piraux, S. Dubois, F. Pailloux, G. Stenuit, J. Govaerts, Physica C 377 (2002) 267.
[14] S. Michotte, S. Mátéfi-Tempfli, L. Piraux, Appl. Phys. Lett. 82 (2003) 4119.
[15] S.K. Lazarouk, A.V. Dolbik, V.A. Labunov, V.E. Borisenko, Physics, Chemistry and Application of Nanostructures, Vol. 223, World Scientific, 2007.
[16] M. Trezza, S.L. Prischepa, C. Cirillo, R. Fittipaldi, M. Sarno, D. Sannino, P. Ciambelli, M.B.S. Hesselberth, S.K. Lazarouk, A.V. Dolbik, V.E. Borisenko, C. Attanasio, J. Appl. Phys. 104 (2008) 083917.
[17] M. Trezza, C. Cirillo, S.L. Prischepa, C. Attanasio, Europhys. Lett. 88 (2009) 57006.
[18] D.S. Hopkins, D. Pekker, P.M. Goldbart, A. Bezryadin, Science 308 (2005) 1762.
[19] C.N. Lau, N. Markovic, M. Bockrath, A. Bezryadin, M. Tinkham, Phys. Rev. Lett. 87 (2001) 217003.
[20] A.V. Herzog, P. Xiong, R.C. Dynes, Phys. Rev. B 58 (1998) 14199.
[21] P. Mikheenko, X. Deng, S. Gildert, M.S. Colclough, R.A. Smith, C.M. Muirhead, P.D. Prewett, J. Teng, Phys. Rev. B 72 (2005) 174506.
[22] A.K. Elmurodov, F.M. Peeters, D.Y. Vodolazov, S. Michotte, S. Adam, F. de Menten de Horne, L. Piraux, D. Lucot, D. Mailly, Phys. Rev. B 78 (2008) 214519.
[23] G.C. Tettamanzi, A. Potenza, S. Rubanov, C.H. Marrows, S. Prawer, Nanotechnology 21 (2010) 168002.